

## PAPER

[View Article Online](#)  
[View Journal](#) | [View Issue](#)

# Thermal stability of $\text{Li}_{1-\Delta}\text{M}_{0.5}\text{Mn}_{1.5}\text{O}_4$ ( $M = \text{Fe}, \text{Co}, \text{Ni}$ ) cathodes in different states of delithiation $\Delta$

Cite this: *RSC Advances*, 2013, **3**, 5909

Aiswarya Bhaskar,<sup>\*abc</sup> Wolfgang Gruner,<sup>b</sup> Daria Mikhailova<sup>†ab</sup> and Helmut Ehrenberg<sup>abc</sup>

The thermal stability of sol-gel synthesized  $\text{Li}_{1-\Delta}\text{M}_{0.5}\text{Mn}_{1.5}\text{O}_4$  ( $M = \text{Fe}, \text{Co}, \text{Ni}$ ) electrodes with different degrees of delithiation were analyzed with TG-DSC and *in situ* synchrotron diffraction under an Ar atmosphere and compared. The onset temperatures for structural degradation are dependent on the amount of lithium  $1-\Delta$  in the sample. The  $\text{Li}_{1-\Delta}\text{Fe}_{0.5}\text{Mn}_{1.5}\text{O}_4$  electrode exhibited the highest thermal stability among the three materials with different dopant  $M$ . The reason for this difference is discussed with respect to the oxidation states of the transition metals. The mechanism of degradation for  $M = \text{Fe}, \text{Co}$  was found to be through gas evolution, mainly  $\text{CO}_2$  and  $\text{O}_2$ , and the carbon conductive additive was found to play a major role in the thermal degradation process. For delithiated  $\text{Li}_{1-\Delta}\text{Ni}_{0.5}\text{Mn}_{1.5}\text{O}_4$  the temperature induced degradation includes phase separation into  $\text{Mn}_3\text{O}_4$  with spinel structure and  $\text{Li}_x\text{Ni}_{1-x}\text{O}$  with rock-salt structure together with oxygen and carbon dioxide release.

Received 25th June 2012,  
Accepted 8th February 2013

DOI: 10.1039/c3ra40356d

[www.rsc.org/advances](http://www.rsc.org/advances)

## Introduction

When battery safety is addressed, thermal stability is a major parameter of consideration. As the temperature inside an electrochemical cell increases, several exothermic reactions such as cathode decomposition and electrolyte oxidation can occur,<sup>1</sup> eventually resulting in a thermal runaway. The Ni substituted  $\text{LiMn}_2\text{O}_4$  spinel,  $\text{LiNi}_{0.5}\text{Mn}_{1.5}\text{O}_4$ , is a candidate for high-power applications and was investigated with respect to its thermal stability in the fully lithiated state ( $\Delta = 0$  in  $\text{Li}_{1-\Delta}\text{Ni}_{0.5}\text{Mn}_{1.5}\text{O}_4$ ) by Pasero *et al.*<sup>2</sup> They have reported that annealing of this material in the completely lithiated state to higher temperatures in air will lead to oxygen release from the spinel lattice, which in turn will lead to a structural degradation. Above  $\sim 750^\circ\text{C}$ , appearance of a rock-salt phase with the  $Fm\bar{3}m$  space group together with the  $Fd\bar{3}m$  spinel phase was observed.<sup>2</sup> Above  $950^\circ\text{C}$ , the amount of this rock-salt phase increases and at  $1100^\circ\text{C}$  the material contains almost single rock-salt phase. Above  $1100^\circ\text{C}$ , a permanent Li loss is reported. These onset temperatures for structural changes should be different in the delithiated states ( $\Delta > 0$ ) and in inert atmospheres. Xiang *et al.* reported in 2009 the

thermal stability of different cathode materials with spinel, olivine and layered structures in contact with  $\text{LiPF}_6$  based electrolyte.<sup>3</sup> According to their observation,  $\text{Li}_{1-\Delta}\text{Ni}_{0.5}\text{Mn}_{1.5}\text{O}_4$  cathode in the delithiated state was showing the worst thermal stability among the cathodes under investigation in the presence of the electrolyte. The onset temperature of decomposition was found to be below  $225^\circ\text{C}$ . Among the tested cathode materials,  $\text{LiFePO}_4$  was showing the best thermal stability and even negligible structural changes after  $300^\circ\text{C}$  in the delithiated state. A work done by Manthiram *et al.* in 2011 on the thermal stability of spinel oxides and oxyfluoride cathodes shows that the Ni substituted spinel cathodes with  $\sim 0.6$  moles of Li in the charged state (corresponding to  $\Delta \sim 0.4$ ) have lower thermal stability in comparison with the completely charged material ( $\Delta \sim 1$ ). This is in disagreement with the general expectation of a monotonously poorer thermal stability with increasing state of charge.<sup>4</sup> They attribute this behavior to the existence of Ni as  $\text{Ni}^{2+}$  in the system. As the  $\text{Ni}^{2+}\text{-O}$  bond is weaker than the  $\text{Mn}^{4+}\text{-O}$  bond, the presence of  $\text{Ni}^{2+}$  weakens the overall bond strength which in turn lowers the activation energy barrier for a thermal decomposition reaction.

The present work is focused on the comparison of the thermal stabilities of citric-acid assisted sol-gel synthesized  $\text{LiM}_{0.5}\text{Mn}_{1.5}\text{O}_4$  ( $M = \text{Fe}, \text{Co}, \text{Ni}$ ) electrode materials, investigated by combined thermogravimetry-differential scanning calorimetry (TG-DSC) and powder diffraction analyses. The structural changes with increasing temperature were investigated under Ar flow for the pure pristine material and cathode mixtures in uncharged ( $\Delta \approx 0$ ), partially ( $\Delta \approx 0.5$ ) and nearly completely charged ( $\Delta \approx 1$ )  $\text{Li}_{1-\Delta}\text{M}_{0.5}\text{Mn}_{1.5}\text{O}_4$  states. The

<sup>a</sup>Institute for Materials Science, Technische Universität Darmstadt, Petersenstr. 23, D-64287, Darmstadt, Germany. E-mail: [aiswarya.bhaskar@kit.edu](mailto:aiswarya.bhaskar@kit.edu)

<sup>b</sup>Institute for Complex Materials, IFW Dresden, Helmholtzstr. 20, D-01069, Dresden, Germany

<sup>c</sup>Karlsruhe Institute of Technology (KIT), Institute for Applied Materials-Energy Storage Systems (IAM-ESS), Hermann-von-Helmholtz-Platz 1, D-76344, Eggenstein-Leopoldshafen, Germany

<sup>†</sup>Present address: Max Planck Institute for Chemical Physics of Solids, Noethnitzer Str. 40, D-01187, Dresden, Germany

onset temperatures of degradation were elucidated and will be discussed.

## Experimental

### Sample preparation

$\text{LiM}_{0.5}\text{Mn}_{1.5}\text{O}_4$  ( $M = \text{Fe}, \text{Co}, \text{Ni}$ ) were synthesized by a citric-acid assisted Pechini process with an annealing at 600 °C for 24 h with intermittent grinding and a post heat treatment at 1000 °C as described elsewhere.<sup>5</sup> The obtained  $\text{LiM}_{0.5}\text{Mn}_{1.5}\text{O}_4$  ( $M = \text{Fe}, \text{Co}$ ) samples are phase pure and belong to the  $Fd\bar{3}m$  space group whereas the  $\text{LiNi}_{0.5}\text{Mn}_{1.5}\text{O}_4$  sample contains in addition a second phase,  $\text{Li}_x\text{Ni}_{1-x}\text{O}$ , which belongs to the  $Fm\bar{3}m$  space group. More details on the structure, morphology and composition were discussed in a previous work.<sup>5</sup> The as-synthesized powders, hereafter will be referred as  $\text{LiM}_{0.5}\text{Mn}_{1.5}\text{O}_4\text{-A}$ , were later used to prepare composite cathodes for the thermal stability studies. The cathode mixture was prepared by grinding the active material with Super P carbon (TIMCAL) and poly(vinylidene difluoride), PVdF 6020, (Solvay Solexis) in a ratio 80 : 10 : 10 in *N*-Methyl Pyrrolidone (Fluka). The mixture was then dried for 3 h in an oven at 100 °C and approximately 80 mg were pressed into a pellet of 12 mm diameter with a pressure of 8 tons. Three pellets were prepared for each material and the prepared pellets were then dried at 120 °C in vacuum for 24 h in a glass oven and weighed. Electrochemical treatments were performed with 1M  $\text{LiPF}_6$  in EC : DMC (ethylene carbonate : dimethyl carbonate, 1 : 1 v/v) electrolyte in Swagelok-cells under conditions similar to the previous work.<sup>5</sup>

The set of the prepared pellets containing a cathode mixture (hereafter will be referred as  $\text{LiM}_{0.5}\text{Mn}_{1.5}\text{O}_4\text{-B}$ ) was used for preparation of other compositions. One part of  $\text{LiM}_{0.5}\text{Mn}_{1.5}\text{O}_4\text{-B}$  was charged till  $\Delta \approx 0.5$  (will be referred as  $\text{Li}_{1-\Delta}\text{M}_{0.5}\text{Mn}_{1.5}\text{O}_4\text{-C}$ ) and another part was charged till  $\Delta \approx 1$  ( $\text{Li}_{1-\Delta}\text{M}_{0.5}\text{Mn}_{1.5}\text{O}_4\text{-D}$ ) for  $M = \text{Fe}, \text{Co}$  and  $\text{Ni}$ , where  $\Delta$  is the number of moles of lithium extracted at a C-rate of C/20. Note that the values for  $\Delta$  in the chemical formulae  $\text{Li}_{1-\Delta}\text{M}_{0.5}\text{Mn}_{1.5}\text{O}_4$  are only approximations of the exact stoichiometry, calculated on the basis of the number of electrons flown and assuming that one Li-ion is extracted per electron. The plots obtained for the partial and complete electrochemical delithiation are shown in Fig. 1. After electrochemical delithiation, the cells were disassembled in an argon-filled box, and the cathodes were washed with DMC (Sigma-Aldrich) to remove the electrolyte residue. The washed cathodes were dried under vacuum in the chamber of the argon-box and ground before any other experiments. The prepared lithiated and delithiated samples were later used for the thermal stability studies. To elucidate more information on the active material, a separate reference test was conducted for a mixture of PVdF binder with Super P carbon only.

### Thermal stability studies – STA

The thermal stability studies were carried out with simultaneous thermogravimetry-differential calorimetric analyses (STA) on the prepared cathode samples with a heating rate

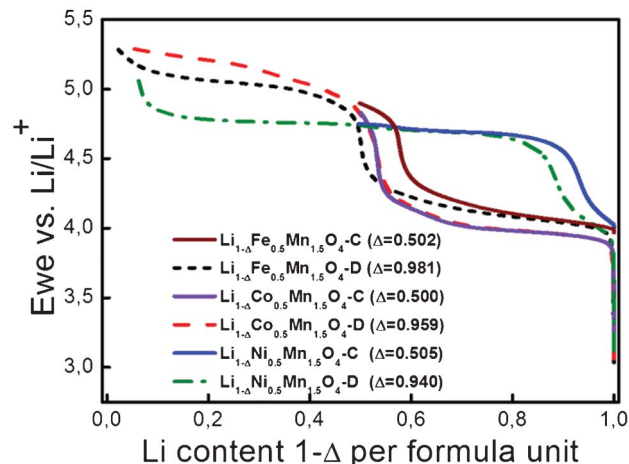


Fig. 1 Voltage (Ewe) vs. number of moles of lithium remaining ( $1-\Delta$ ) plots, showing complete ( $\Delta \approx 1$ ) and partial delithiation ( $\Delta \approx 0.5$ ) of the samples used for thermal stability studies.

of 10 °C  $\text{min}^{-1}$  under Ar atmosphere using a Model STA 449 apparatus (Netzsch, Germany). Samples in an alumina crucible (for differential thermal analysis, DTA, mode) or Pt-Rh crucible (for DSC mode) were heated to the specified temperature. Simultaneously, the quadrupole mass spectrometer (QMS) Prisma (Pfeiffer Vacuum, Germany) was coupled with the thermoanalyzer device to detect evolved gases during heating.

### X-Ray powder diffraction

All prepared samples were analyzed by X-ray diffraction (XRD) with a STOE STADI/P powder diffractometer [ $\text{Mo-K}\alpha_1$  radiation, curved Ge(111) monochromator, step width 0.02° ( $2\theta$ ), linear position sensitive detector]. The as-prepared samples were analyzed in a flat-sample transmission mode, while the delithiated samples were analyzed in Debye-Scherrer mode using capillaries, sealed under Ar atmosphere. Changes in the underlying crystal structures were detected by XRD analyses on samples before and after the thermal treatment (*ex situ*). For a more detailed investigation of the thermal evolution of phase compositions and structures, *in situ* synchrotron diffraction was performed during heating.

### Synchrotron powder diffraction at elevated temperatures

Structural investigations of  $\text{LiNi}_{0.5}\text{Mn}_{1.5}\text{O}_4$  (-A, -B, -D) and  $\text{Li}_{1-\Delta}\text{Co}_{0.5}\text{Mn}_{1.5}\text{O}_4$  (-C, -D) samples have been performed over a temperature range of 22–300 °C by synchrotron diffraction at beamline B2<sup>6</sup> of the synchrotron facility Hamburger Synchrotronstrahlungslabor HASYLAB at Deutsches Elektronen-Synchrotron DESY (Hamburg, Germany). The diffraction patterns were recorded in Debye-Scherrer mode using the on-site readable image-plate detector OBI,<sup>7</sup> a STOE furnace equipped with a EUROTHERM temperature controller and a capillary spinner. 0.3 mm glass capillaries were filled with powdered samples in a glove-box under Ar atmosphere, sealed and mounted inside the STOE furnace. The data were collected in steps of 0.004° from  $2\theta = 5\text{--}60^\circ$  in temperature

steps of 20 °C. The wavelength of 0.73048(1) Å was selected by a double-crystal monochromator and determined from the positions of 8 reflections from a LaB<sub>6</sub> reference material.

All diffraction patterns have been analyzed by using the software package WinPLOTR, including the Rietveld refinement program FullProf.<sup>8</sup> For structure determination, a full-profile Rietveld refinement of the crystal and microstructure parameters was performed with an isotropic approximation for thermal displacement. The standard deviations of refined parameters were calculated in agreement with Berar and Lelann.<sup>9</sup> Crystallite sizes were refined by taking the instrumental resolution function, determined for a LaB<sub>6</sub> powder reference material, explicitly into account.

## Results and discussion

### Structural characterization of the samples

X-Ray analysis revealed the preservation of the spinel structure in the *Fd3m* space group after partial and complete delithiation. The completely delithiated Li<sub>1-Δ</sub>Ni<sub>0.5</sub>Mn<sub>1.5</sub>O<sub>4</sub>-D sample contains two spinel phases, one with a smaller (82% w/w) and one with a larger (6% w/w) lattice parameter, together with about 12% (w/w) of rock-salt type Li<sub>x</sub>Ni<sub>1-x</sub>O. The XRD patterns of the Li<sub>1-Δ</sub>M<sub>0.5</sub>Mn<sub>1.5</sub>O<sub>4</sub>-C and Li<sub>1-Δ</sub>M<sub>0.5</sub>Mn<sub>1.5</sub>O<sub>4</sub>-D samples are shown in Fig. 2 together with the calculated profiles after Rietveld refinement. A comparison of the lattice parameters of the samples Li<sub>1-Δ</sub>M<sub>0.5</sub>Mn<sub>1.5</sub>O<sub>4</sub>-B, Li<sub>1-Δ</sub>M<sub>0.5</sub>Mn<sub>1.5</sub>O<sub>4</sub>-C and Li<sub>1-Δ</sub>M<sub>0.5</sub>Mn<sub>1.5</sub>O<sub>4</sub>-D is given in Table 1a. This comparison

**Table 1** The room temperature lattice parameters obtained from XRD analysis (a) of Li<sub>1-Δ</sub>M<sub>0.5</sub>Mn<sub>1.5</sub>O<sub>4</sub> (M = Fe, Co, Ni)-B, -C and Li<sub>1-Δ</sub>M<sub>0.5</sub>Mn<sub>1.5</sub>O<sub>4</sub>-D samples a) before and b) after the thermal stability experiments up to 350 °C. The results for the two spinel phases in the Li<sub>1-Δ</sub>Ni<sub>0.5</sub>Mn<sub>1.5</sub>O<sub>4</sub>-D samples are reported together. The first value refers to the phase with the higher content

#### a) Before heating

M	Sample B a/Å	Sample C a/Å	Sample D a/Å
Fe	8.2705(2)	8.1652(5)	8.0894(6)
Co	8.1632(3)	8.0572(6)	8.0283(5)
Ni	8.1955(4)	8.1035(4)	8.109(2)/8.0105(4)

#### b) After heating

M	Sample B a/Å	Sample C a/Å	Sample D a/Å
Fe	8.2605(3)	8.190(2)	8.118(9)
Co	8.1485(3)	8.143(2)	8.085(2)
Ni	8.1899(3)	8.1642(7)	8.133(1)/8.033(1)

shows the unit cells' shrinking about 1.27%, 1.30% and 1.12% in the case of Fe-, Co- and Ni-doped "C" samples, respectively and 2.19%, 1.65% and 2.26% (for the LiNi<sub>0.5</sub>Mn<sub>1.5</sub>O<sub>4</sub> phase with 82% w/w in the sample) in the case of Fe-, Co- and Ni-doped "D" samples, respectively, as a result of the Li extraction.

### Thermal stability studies

The high temperature studies were performed for Li<sub>1-Δ</sub>M<sub>0.5</sub>Mn<sub>1.5</sub>O<sub>4</sub>-B, C and Li<sub>1-Δ</sub>M<sub>0.5</sub>Mn<sub>1.5</sub>O<sub>4</sub>-D samples (M = Fe, Co, Ni). The thermal analysis measurements performed for the carbon-binder system alone are shown in Fig. 3, the other results of the thermogravimetric analyses in Fig. 4.

An endothermic peak at ~160 °C could be related to the melting of the binder PVdF as there was no weight change observed in the TG curve. This endothermic peak was observed for all the samples containing the electrochemically active material analyzed later because these samples contain 10% w/w of PVdF. It was also found that the PVdF sample undergoes decomposition after 370 °C, as revealed by the weight loss and the evolution of decomposition gases (*m/z* 18, 32 and 44) at this temperature in the STA-QMS analysis. Therefore, the

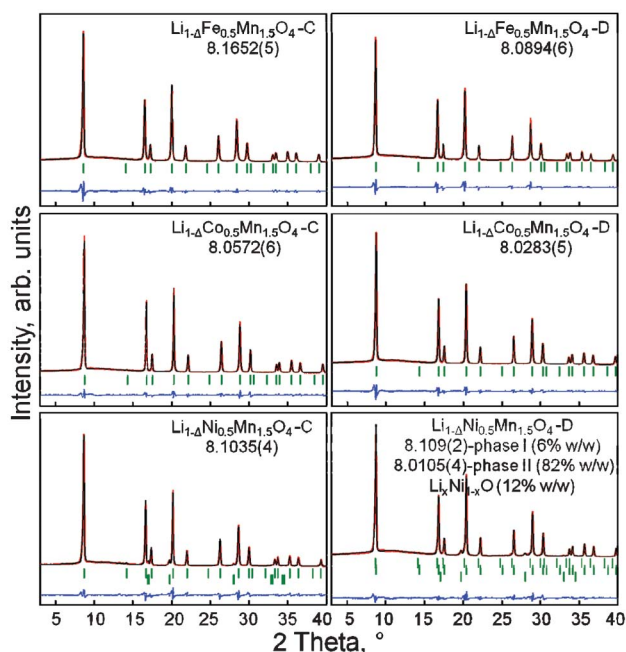


**Fig. 2** RT XRD patterns obtained for LiM<sub>0.5</sub>Mn<sub>1.5</sub>O<sub>4</sub> (M = Fe, Co, Ni) after partial (left) and complete (right) electrochemical delithiation. The corresponding lattice parameters (in Å) are given in the inset of each figure. The last line of reflection marks in the LiNi<sub>0.5</sub>Mn<sub>1.5</sub>O<sub>4</sub> samples corresponds to the Li<sub>x</sub>Ni<sub>1-x</sub>O phase (*Fm3m* space group).

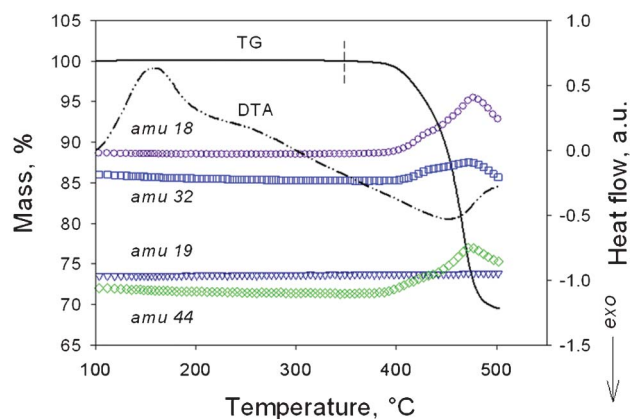


**Fig. 3** TG, DTA, and simultaneous QMS signals for species with selected molar masses (*m/z* 18, 19, 32 and 44) of the carbon-PVdF mixture.

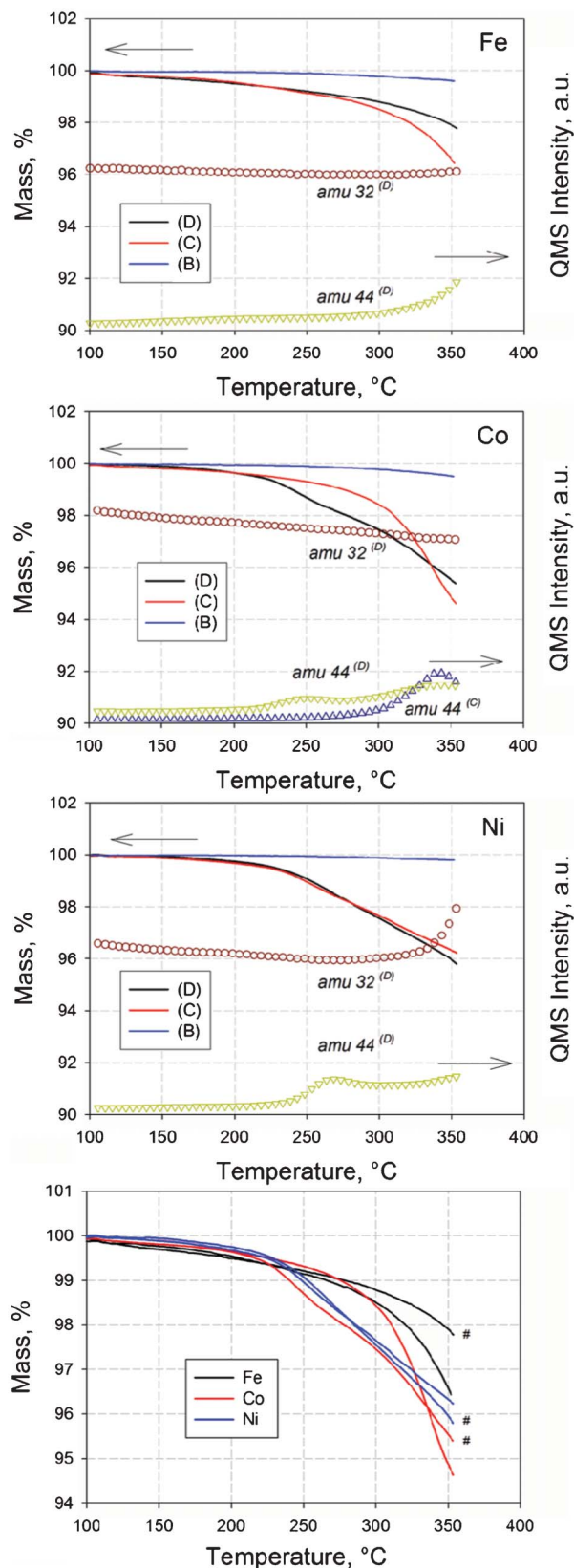


**Fig. 4** TG and selected simultaneous QMS signals for samples of the series "B", "C", and "D". The TG signals after partial and complete (#) delithiation are distinct by hash marks.

thermal stability studies of the cathode materials were limited to a maximum temperature of 350 °C to avoid binder decomposition. The sensitivity of DTA is lower, and for the small available amount of electrochemically treated material, DSC measurements were performed on these samples instead. The comparison of thermo-analytical results and mass spectrometry from these two techniques are therefore only semi-quantitative.

Only less than 0.5% weight loss was observed until 350 °C for the initial electrode mixtures ( $\text{LiM}_{0.5}\text{Mn}_{1.5}\text{O}_4\text{-B}$ ), whereas more pronounced weight losses were observed for the  $\text{Li}_{1-\Delta}\text{M}_{0.5}\text{Mn}_{1.5}\text{O}_4\text{-C}$  and  $\text{D}$  samples (Fig. 4). The weight losses of about 0.5% were observed below 200 °C for both electrochemically treated samples of C- and D-types, which could be attributed to the loss of traces of  $\text{LiPF}_6$  or other contaminants like surface films which were not completely removed by the washing with DMC.<sup>1</sup> The differences in STA measurements above 200 °C reflect the different thermal stabilities of the three series of samples "B", "C" and "D":

1) Considering the set of partially delithiated  $\text{Li}_{1-\Delta}\text{M}_{0.5}\text{Mn}_{1.5}\text{O}_4\text{-C}$  samples, the weight losses increase at about ~200 °C and reach values of about 2.0%, 5.0% and 3.3% at 350 °C for the Fe-, Co- and Ni-doped samples, respectively. The weight losses are accompanied by small exothermic DSC signals for Co and Ni with maxima around 330 °C and 250 °C, respectively, while no such signal was observed for the Fe doped sample.

2) The completely delithiated  $\text{Li}_{1-\Delta}\text{Fe}_{0.5}\text{Mn}_{1.5}\text{O}_4\text{-D}$  sample showed a mass loss from 200 °C, similar to the behavior of the partially delithiated sample. No characteristic DSC signals were observed, but a weak  $\text{CO}_2$  signal ( $m/z$  44) was detected by QMS above 300 °C.

3) In contrast to a gradual mass change as for the partially delithiated  $\text{Li}_{1-\Delta}\text{Co}_{0.5}\text{Mn}_{1.5}\text{O}_4\text{-C}$  sample, a pronounced step-like mass loss is visible from ~220 °C, accompanied by an exothermic signal and a simultaneous detection of  $\text{CO}_2$  for completely delithiated  $\text{Li}_{1-\Delta}\text{Co}_{0.5}\text{Mn}_{1.5}\text{O}_4\text{-D}$ . Above 300 °C a significant increase of the  $\text{CO}_2$  release was detected in both  $\text{Li}_{1-\Delta}\text{Co}_{0.5}\text{Mn}_{1.5}\text{O}_4\text{-C}$  and  $\text{-D}$  samples.

4) The nearly constant mass losses in the TG curves of partially delithiated  $\text{Li}_{1-\Delta}\text{Ni}_{0.5}\text{Mn}_{1.5}\text{O}_4\text{-C}$  and fully delithiated  $\text{Li}_{1-\Delta}\text{Ni}_{0.5}\text{Mn}_{1.5}\text{O}_4\text{-D}$  are very similar. The maximum of the DSC signal at ~240 °C for  $\text{Li}_{1-\Delta}\text{Ni}_{0.5}\text{Mn}_{1.5}\text{O}_4\text{-D}$  is shifted several degrees to higher temperature in comparison with that of  $\text{Li}_{1-\Delta}\text{Ni}_{0.5}\text{Mn}_{1.5}\text{O}_4\text{-C}$ . The corresponding mass loss reaction is accompanied by a  $\text{CO}_2$  ( $m/z$  44) detection. Interestingly, only the completely delithiated  $\text{Li}_{1-\Delta}\text{Ni}_{0.5}\text{Mn}_{1.5}\text{O}_4\text{-D}$  sample showed the evolution of oxygen ( $m/z$  32) at temperatures above 300 °C.

From the above observations it can be concluded that the thermal stability of  $\text{Li}_{1-\Delta}\text{M}_{0.5}\text{Mn}_{1.5}\text{O}_4$  ( $M = \text{Fe}, \text{Co}, \text{Ni}$ ) is mainly related to the state of charge and differs depending on the  $M$  element. This difference in the thermal stability could be attributed to the presence of the higher oxidation states of transition metals which tend to change to stable lower oxidation states by releasing oxygen from the structure. As a result, the structure of the materials could degrade, and materials undergo phase changes. The oxygen release leads partially to the oxidation of conductive additive to form  $\text{CO}_2$ .

Among the three  $\text{Li}_{1-\Delta}\text{M}_{0.5}\text{Mn}_{1.5}\text{O}_4$  ( $M = \text{Fe, Co, Ni}$ ) materials,  $\text{Li}_{1-\Delta}\text{Fe}_{0.5}\text{Mn}_{1.5}\text{O}_4$  was found to exhibit the highest thermal stability in both the charged and discharged states. This difference could be explained based on the distribution of oxidation states in these materials. The Ni-doped material contains in its completely stoichiometric and fully lithiated form Ni in its divalent state and Mn in its tetravalent state.<sup>10</sup> A small oxygen deficiency in these materials results in the presence of some Mn in its trivalent form.<sup>11</sup> The relative  $\text{Mn}^{3+}/\text{Mn}^{4+}$  ratio for these systems can be obtained from the capacities in the 4V region of the GCPL-curves (Fig. 1), where only Mn is electrochemically active. As calculated,  $\text{LiNi}_{0.5}\text{Mn}_{1.5}\text{O}_4\text{-A}$  contains  $\sim 0.08$  moles and  $\text{LiM}_{0.5}\text{Mn}_{1.5}\text{O}_4\text{-A}$  ( $M = \text{Fe, Co}$ ) contains  $\sim 0.35$  moles of trivalent Mn per one mole of the  $\text{LiM}_{0.5}\text{Mn}_{1.5}\text{O}_4$  material. When completely charged, Mn and  $M$  (Fe, Co, Ni) in  $\text{LiM}_{0.5}\text{Mn}_{1.5}\text{O}_4\text{-D}$  ( $M = \text{Fe, Co, Ni}$ ) reach their tetravalent oxidation states.<sup>12,13</sup> For the partially charged materials, all Mn is in its tetravalent oxidation state, whereas the oxidation states of  $M$  are different for  $M = \text{Fe, Co}$  and Ni. While most of the Fe and Co still remains in their trivalent states, Ni is already oxidized to  $\text{Ni}^{3+}$  or a  $\text{Ni}^{2+}/\text{Ni}^{4+}$  mixture (see oxidation plateaus in Fig. 1). The different stabilities of these oxidation states are most probably responsible for the degradation of partially and fully delithiated  $\text{Li}_{1-\Delta}\text{M}_{0.5}\text{Mn}_{1.5}\text{O}_4$  and  $\text{Li}_{1-\Delta}\text{M}_{0.5}\text{Mn}_{1.5}\text{O}_4$  ( $M = \text{Ni, Co}$ ) at lower temperatures than for  $M = \text{Fe}$ .

Accordingly, with increasing delithiation, *i.e.* high values of  $\Delta$ , the onset temperature for its decomposition decreases, except for the  $\text{Li}_{1-\Delta}\text{Ni}_{0.5}\text{Mn}_{1.5}\text{O}_4\text{-C}$  sample.<sup>1</sup> Previous reports also agree to the above observation of less thermal stability of Ni containing systems and higher thermal stability of  $\text{Li}_{1-\Delta}\text{Ni}_{0.5}\text{Mn}_{1.5}\text{O}_4\text{-D}$  ( $\Delta \sim 1$ ) over the  $\text{Li}_{1-\Delta}\text{Ni}_{0.5}\text{Mn}_{1.5}\text{O}_4\text{-C}$  sample ( $\Delta \sim 0.5$ ) in contrast to the normal trend of less stability with increasing state of charge.<sup>3,4</sup>

### Characterization of the samples after TG-DSC analyses

The XRD analyses for the  $\text{LiM}_{0.5}\text{Mn}_{1.5}\text{O}_4\text{-B}$  samples after the TG-DSC studies up to 350 °C are shown in Fig. 5. Note that after cooling back to RT all samples show a decrease in the lattice parameters in comparison with their initial states before the heat treatment (see Table 1b). Therefore, minor changes in the crystal structure took place, which are only reflected in very small shifts of the positions of the Bragg reflections, but without significant changes in their intensities.

The  $\text{Li}_{1-\Delta}\text{M}_{0.5}\text{Mn}_{1.5}\text{O}_4\text{-C}$  and  $\text{Li}_{1-\Delta}\text{M}_{0.5}\text{Mn}_{1.5}\text{O}_4\text{-D}$  samples show significant increases in the lattice parameters after heat treatment under argon up to 350 °C, as revealed by the XRD analysis. The increases in the cell parameters confirm that oxygen losses from the lattices are the major cause of structural degradation of these materials. Another important observation is the appearance of additional reflections (marked by “\*” in Fig. 6) in the patterns after the thermal treatment for  $M = \text{Ni}$  and Co, which is more pronounced for the completely charged samples “D”. The newly formed phases do not match to any of the known phases, which are included in the data base of the ICDD.<sup>15</sup>

A list of the d-spacings for the additional reflections is given in Table 2. From the XRD results of delithiated samples one

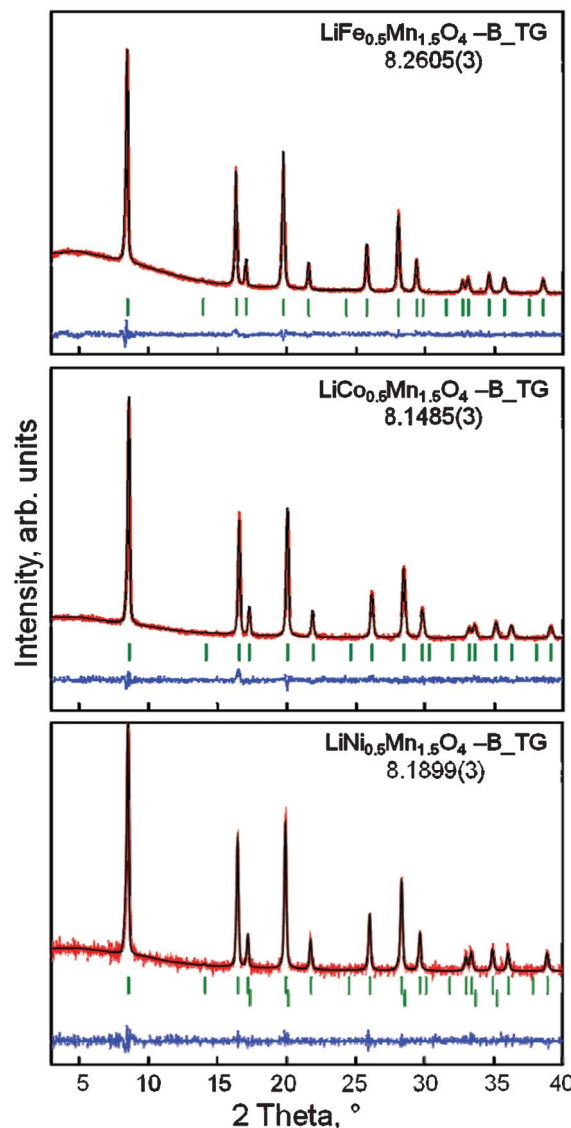


**Fig. 5** RT XRD patterns obtained for  $\text{LiM}_{0.5}\text{Mn}_{1.5}\text{O}_4\text{-B}$  ( $M = \text{Fe, Co, Ni}$ ) after heating under argon at a rate of  $10\text{ °C min}^{-1}$  up to 350 °C and cooling down to RT. The corresponding lattice parameters (in Å) are given in the inset of each figure. The last line of reflection marks in the  $\text{LiNi}_{0.5}\text{Mn}_{1.5}\text{O}_4\text{-B}$  sample corresponds to the  $\text{Li}_x\text{Ni}_{1-x}\text{O}$  phase ( $Fm\bar{3}m$  space group).

can conclude that the thermal stability of  $\text{LiM}_{0.5}\text{Mn}_{1.5}\text{O}_4\text{-A}$  ( $M = \text{Fe, Co, Ni}$ ) spinel cathode materials is related to the onset of oxygen release from the lattices.

### In situ structural analyses

To extract more information on the degradation mechanism, *in situ* synchrotron diffraction investigations were carried out during heating in Ar. Ni and Co substituted samples were selected for this purpose, because they are unstable in their delithiated states in comparison with the Fe substituted sample. The  $\text{LiNi}_{0.5}\text{Mn}_{1.5}\text{O}_4\text{-A}$  sample was thermally stable until 300 °C exhibiting only a spinel phase and a small amount of  $\text{Li}_x\text{Ni}_{1-x}\text{O}$  similar to the synthesis product. The lattice

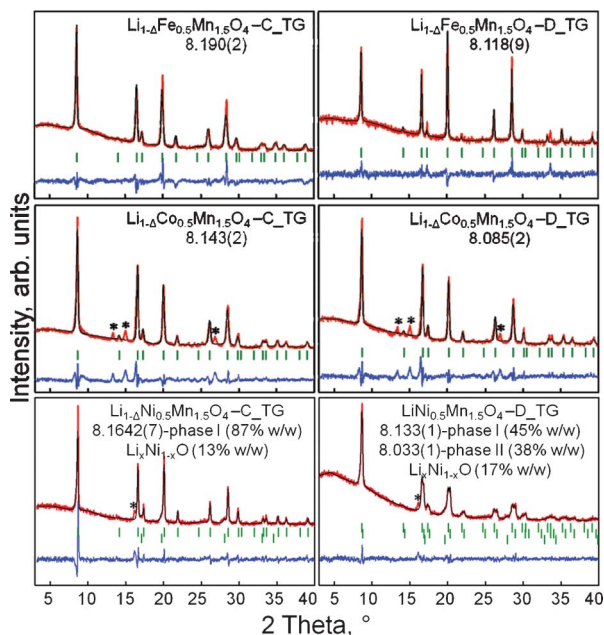


**Fig. 6** RT XRD patterns obtained for  $\text{Li}_{1-\Delta}\text{M}_{0.5}\text{Mn}_{1.5}\text{O}_4$ -C ( $M = \text{Fe, Co, Ni}$ ) on the left from top to bottom and for  $\text{Li}_{1-\Delta}\text{M}_{0.5}\text{Mn}_{1.5}\text{O}_4$ -D ( $M = \text{Fe, Co, Ni}$ ). All experiments were performed at room temperature after an intermediate heating under argon at a rate of  $10\text{ }^\circ\text{C min}^{-1}$  up to  $350\text{ }^\circ\text{C}$ . The corresponding lattice parameters (in Å) are given in the inset of each figure. The last line of reflection marks in the  $\text{LiNi}_{0.5}\text{Mn}_{1.5}\text{O}_4$  samples corresponds to the  $\text{Li}_x\text{Ni}_{1-x}\text{O}$  phase ( $Fm\bar{3}m$  space group).

parameter evolution of  $\text{LiNi}_{0.5}\text{Mn}_{1.5}\text{O}_4$ -A during heating is shown in Fig. 7a.

For the  $\text{LiNi}_{0.5}\text{Mn}_{1.5}\text{O}_4$ -B sample, a formation of the second spinel phase with the same cubic symmetry but a larger lattice parameter was observed at elevated temperatures, see Fig. 7b. These two phases could exhibit different cation stoichiometry or different cation distribution, but most probably a partial reduction of  $\text{LiNi}_{0.5}\text{Mn}_{1.5}\text{O}_4$  takes place in the argon atmosphere in presence of amorphous carbon. This results in an increase of the lattice parameters. Diffraction patterns starting from  $240\text{ }^\circ\text{C}$  can be explained based on the model with two spinel phases with slightly different lattice parameters, probably due to an inhomogeneous distribution of oxygen in the crystallites (see Fig. 7d) which resulted from the partial reduction of the material. A difference in the thermal behavior of  $\text{LiNi}_{0.5}\text{Mn}_{1.5}\text{O}_4$ -A and  $\text{LiNi}_{0.5}\text{Mn}_{1.5}\text{O}_4$ -B samples reveals the role of carbon as a reducing agent in the thermal degradation of electrode materials.

The diffraction pattern of  $\text{Li}_{1-\Delta}\text{Ni}_{0.5}\text{Mn}_{1.5}\text{O}_4$ -D can be described at room temperature based on two spinel phases (space group  $Fd\bar{3}m$ ) with slightly different lattice parameters  $a = 8.0065(1)\text{ Å}$  and  $a = 8.0169(3)\text{ Å}$ , and a small amount of cubic  $\text{Li}_x\text{Ni}_{1-x}\text{O}$  (less than 4% w/w). These two spinel phases should have a small difference in the lithium content as a result of inhomogeneous charging. The phase with more lithium should have a larger unit cell. Above  $220\text{ }^\circ\text{C}$  a third cubic spinel phase with lattice parameter  $a = 8.4295(7)\text{ Å}$  appears at  $300\text{ }^\circ\text{C}$  which is similar to the reported lattice parameter for high-temperature spinel form of  $\text{Mn}_3\text{O}_4$  in literature ( $a = 8.42\text{ Å}^{14}$ ) see Fig. 7c. At the same time the lattice parameter of the second spinel phase increases significantly, and the  $\text{Li}_x\text{Ni}_{1-x}\text{O}$  content in the sample increases from 3.5% up to 32% w/w. These facts point out a complicated character of degradation for the delithiated  $\text{Li}_{1-\Delta}\text{Ni}_{0.5}\text{Mn}_{1.5}\text{O}_4$  sample ( $\Delta \sim 1$ ) at elevated temperatures under reducing conditions. Together with oxygen release a phase separation due to cation diffusion takes place, leading to the formation of a  $\text{Mn}_3\text{O}_4$ -like spinel phase with a small Li-content and  $\text{Li}_x\text{Ni}_{1-x}\text{O}$  with rock-salt type structure. While temperature increases, the amount of  $\text{Li}_{z_1}\text{Ni}_{0.5}\text{Mn}_{1.5}\text{O}_4$  (where “z” replaces  $1-\Delta$ ) with a larger unit cell, which corresponds to more Li in the sample, decreases faster than the amount of  $\text{Li}_{z_2}\text{Ni}_{0.5}\text{Mn}_{1.5}\text{O}_4$  with a smaller unit cell and less Li in the sample ( $z_2 < z_1$ ). It means that among the charged samples, the phase with less lithium content seems to be more stable against thermal decomposition and reduction. This is in well agreement with the DSC results of delithiated  $\text{Li}_{1-\Delta}\text{Ni}_{0.5}\text{Mn}_{1.5}\text{O}_4$  samples, where the partially delithiated material had a lower onset temperature of degradation than the completely charged material. The lower stability of partially delithiated material could be due to the presence of  $\text{Ni}^{2+}$  and  $\text{Ni}^{4+}$  with quite different ionic radii simultaneously, while completely delithiated material contains only  $\text{Ni}^{4+}$ . Additional information about oxidation states of Ni in partially delithiated samples is required to confirm this supposition.

In contrast to  $\text{Li}_{1-\Delta}\text{Ni}_{0.5}\text{Mn}_{1.5}\text{O}_4$ -D, the two samples  $\text{Li}_{1-\Delta}\text{Co}_{0.5}\text{Mn}_{1.5}\text{O}_4$ -C and  $\text{Li}_{1-\Delta}\text{Co}_{0.5}\text{Mn}_{1.5}\text{O}_4$ -D show more simple degradation behaviors up to  $300\text{ }^\circ\text{C}$  without changes in the cation distribution. The appearance of a second spinel phase with larger lattice parameter starts from  $\sim 250\text{ }^\circ\text{C}$  for  $\text{Li}_{1-\Delta}\text{Co}_{0.5}\text{Mn}_{1.5}\text{O}_4$ -C and from  $\sim 190\text{ }^\circ\text{C}$  for the  $\text{Li}_{1-\Delta}\text{Co}_{0.5}\text{Mn}_{1.5}\text{O}_4$ -D sample (see Fig. 8a and b). This behavior is in agreement with the observation from TG analysis and differs from that of the  $\text{Li}_{1-\Delta}\text{Ni}_{0.5}\text{Mn}_{1.5}\text{O}_4$ -D sample with phase separation and lower onset temperature of degradation for the partially charged samples as also revealed from TGA.

Hence it can be concluded that the degradation of the materials proceeds *via* oxygen release from the lattice for delithiated  $\text{Li}_{1-\Delta}\text{Co}_{0.5}\text{Mn}_{1.5}\text{O}_4$  and oxygen release and phase separation for delithiated  $\text{Li}_{1-\Delta}\text{Ni}_{0.5}\text{Mn}_{1.5}\text{O}_4$  samples within the investigated temperature range. The onset temperature of degradation is lower for a partially delithiated state in comparison with the fully lithiated state  $\text{LiCo}_{0.5}\text{Mn}_{1.5}\text{O}_4$ . However, these experiments were performed in the absence of any electrolytes. It is known that the  $\text{LiPF}_6$  based electrolytes undergo exothermic reactions below  $225\text{ }^\circ\text{C}$  which results from the ring opening reactions of ethylene carbonate into

**Table 2** d-Values (in Å) of the strongest additional reflections observed after thermal excursion to  $350\text{ }^\circ\text{C}$  in partially or fully delithiated states

M	Sample C	Sample D
Fe	None	None
Co	3.057, 2.716, 1.529	3.042, 2.706, 1.521
Ni	2.522	2.530

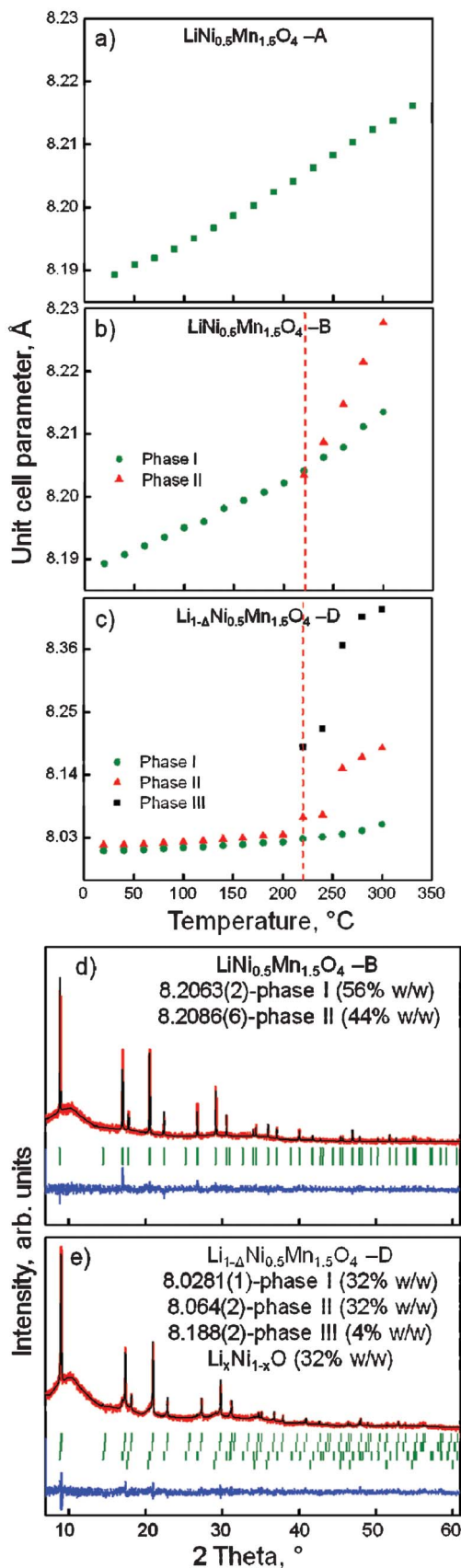


**Fig. 7** Temperature dependence  $a(T)$  of the cubic lattice parameter, obtained from *in situ* synchrotron diffraction analyses ( $\lambda = 0.73048(1) \text{ \AA}$ ) for a)  $\text{LiNi}_{0.5}\text{Mn}_{1.5}\text{O}_4\text{-A}$ . b)  $\text{LiNi}_{0.5}\text{Mn}_{1.5}\text{O}_4\text{-B}$  and c) spinel phases of  $\text{Li}_{1-\Delta}\text{Ni}_{0.5}\text{Mn}_{1.5}\text{O}_4\text{-D}$ . Close to 240 °C for  $\text{LiNi}_{0.5}\text{Mn}_{1.5}\text{O}_4\text{-B}$ , a partial reduction of the phase takes place, which is reflected in the different slope of the temperature dependence. Close to 220 °C for  $\text{Li}_{1-\Delta}\text{Ni}_{0.5}\text{Mn}_{1.5}\text{O}_4\text{-D}$ , the appearance of a third spinel phase together with the significant increasing of the lattice parameters of the other spinel phases was observed. d) Diffraction pattern at 240 °C for the  $\text{LiNi}_{0.5}\text{Mn}_{1.5}\text{O}_4\text{-B}$  sample, where the second spinel phase appears. e) Diffraction pattern at 220 °C for  $\text{Li}_{1-\Delta}\text{Ni}_{0.5}\text{Mn}_{1.5}\text{O}_4\text{-D}$ , where the third spinel phase appears. The last line of reflection marks corresponds to the  $\text{Li}_x\text{Ni}_{1-x}\text{O}$  phase with 32% w/w ( $Fm\bar{3}m$  space group).

polymeric products. As mentioned in the introduction part of the manuscript, the nature of the cathode materials has a big influence on the onset temperature of these reactions. Especially an oxygen release from the electrode at lower temperature would promote this electrolyte decomposition much earlier. Also it is known that systems containing Mn have lower onset temperatures in the presence of electrolytes due to the dissolution of Mn-ions in the electrolyte which is further influenced by the structural instability of the electrode materials.<sup>1,3,16</sup> Hence in the presence of electrolyte the onset

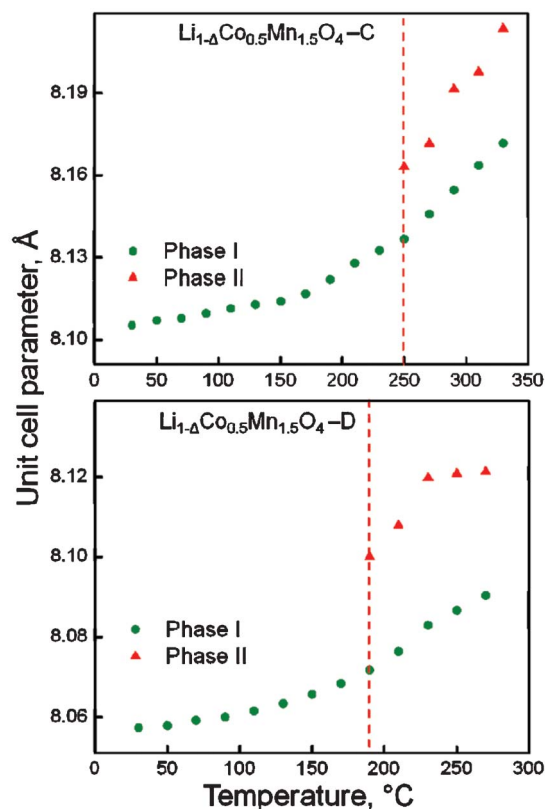


**Fig. 8** Temperature dependence of the cubic lattice parameter, obtained from *in situ* synchrotron diffraction analyses ( $\lambda = 0.73048(1) \text{ \AA}$ ), for spinel phases of (a)  $\text{Li}_{1-\Delta}\text{Co}_{0.5}\text{Mn}_{1.5}\text{O}_4\text{-C}$  and (b)  $\text{Li}_{1-\Delta}\text{Co}_{0.5}\text{Mn}_{1.5}\text{O}_4\text{-D}$ . Close to 250 °C for  $\text{Li}_{1-\Delta}\text{Co}_{0.5}\text{Mn}_{1.5}\text{O}_4\text{-C}$  and 190 °C for  $\text{Li}_{1-\Delta}\text{Co}_{0.5}\text{Mn}_{1.5}\text{O}_4\text{-D}$ , the appearance of the second spinel phase together with significant increases of the lattice parameters were observed.

temperature of degradation of the electrode–electrolyte system could be even much more reduced.

## Summary and conclusions

Thermal stability studies of the  $\text{Li}_{1-\Delta}\text{M}_{0.5}\text{Mn}_{1.5}\text{O}_4$  ( $M = \text{Fe}, \text{Co}, \text{Ni}$ ) cathodes were conducted using combined TG-DSC analysis. The onset temperature is found to be lowest for the completely charged samples ( $\Delta \approx 1$ ) and slightly higher for the partially charged samples ( $\Delta \approx 0.5$ ) except in the case of  $\text{LiNi}_{0.5}\text{Mn}_{1.5}\text{O}_4$ . The reason of the lower stability of completely charged  $\text{Li}_{1-\Delta}\text{M}_{0.5}\text{Mn}_{1.5}\text{O}_4\text{-D}$  ( $M = \text{Fe}, \text{Co}$ ) could be the existence of most of the transition metal ions in their tetravalent form in the charged states. These ions tend to get reduced to their stable valences mainly by releasing oxygen from the structural framework. The released oxygen in turn reacts with the carbon present in the cathode and degrades the composite by expelling carbon dioxide. Hence it can be concluded that the thermal stability is directly related to the amount of lithium in the samples for  $\text{Li}_{1-\Delta}\text{M}_{0.5}\text{Mn}_{1.5}\text{O}_4$  ( $M = \text{Fe}, \text{Co}$ ). *In situ* synchrotron diffraction studies performed for uncharged Ni doped spinel in presence of amorphous carbon showed that the material starts to release oxygen above  $\sim 240^\circ\text{C}$ , and a cubic spinel phase with a larger unit cell forms. The investigations of the completely charged Ni-doped spinel revealed an onset temperature of  $\sim 220^\circ\text{C}$ . The degradation of the delithiated Ni-containing spinel includes oxygen release together with phase separation leading to the formation of a  $\text{Mn}_3\text{O}_4$ -like phase and  $\text{Li}_x\text{Ni}_{1-x}\text{O}$ . Similar studies on  $\text{Li}_{1-\Delta}\text{Co}_{0.5}\text{Mn}_{1.5}\text{O}_4$  samples showed a formation of only the second spinel phase with a larger unit cell during increasing temperature, *i.e.* close to  $250^\circ\text{C}$  and  $190^\circ\text{C}$  respectively for the partially and completely delithiated samples. No phase separation into  $\text{Mn}_3\text{O}_4$  and  $\text{CoO}$  was observed, confirming the different degradation mechanisms for Ni- and Co-containing spinels at elevated temperature in charged states.

## Acknowledgements

Financial support by the “Deutsche Forschungsgemeinschaft” (DFG, EH183/8) is gratefully acknowledged. This work has benefited from beam time allocation by HASYLAB at beamline B2. The authors thank T. Leiter and A. Sarapulova for the help in sample preparation, C. Geringswald for the thermoanalytical measurements and N. N. Bramnik for the initial support in this work.

## References

- 1 Q. Wang, J. Sun and C. Chen, *J. Electrochem. Soc.*, 2007, **154**, A263–A267.
- 2 D. Pasero, N. Reeves, V. Pralong and A. R. West, *J. Electrochem. Soc.*, 2008, **155**, A282–A291.
- 3 H. F. Xiang, H. Wang, C. H. Chen, X. W. Ge, S. Guo, J. H. Sun and W. Q. Hu, *J. Power Sources*, 2009, **191**, 575–581.
- 4 K. R. Stroukoff and A. Manthiram, *J. Mater. Chem.*, 2011, **21**, 10165–10170.
- 5 A. Bhaskar, N. N. Bramnik, A. Senyshyn, H. Fuess and H. Ehrenberg, *J. Electrochem. Soc.*, 2010, **157**, A689–A695.
- 6 M. Knapp, C. Baetz, H. Ehrenberg and H. Fuess, *J. Synchrotron Radiat.*, 2004, **11**, 328–334.
- 7 M. Knapp, V. Joco, C. Baetz, H. H. Brecht, A. Berghaeuser, H. Ehrenberg, H. von Seggern and H. Fuess, *Nucl. Instrum. Methods Phys. Res., Sect. A*, 2004, **521**, 565–570.
- 8 T. Roisnel and J. Rodriguez-Carvajal, *Mater. Sci. Forum*, 2001, **378–381**, 118–123.
- 9 J. F. Berar and P. Lelann, *J. Appl. Crystallogr.*, 1991, **24**, 1–5.
- 10 J.-H. Kim, C. S. Yoon, S.-T. Myung, J. Prakash and Y.-K. Sun, *Electrochem. Solid-State Lett.*, 2004, **7**, A216–A220.
- 11 Q. Zhong, A. Bonakdarpour, M. Zhang, Y. Gao and J. R. Dahn, *J. Electrochem. Soc.*, 1997, **144**, 205–213.
- 12 T. Ohzuku, K. Ariyoshi, S. Takeda and Y. Sakai, *Electrochim. Acta*, 2001, **46**, 2327–2336.
- 13 P. Aitchison, B. Ammundsen, D. J. Jones, G. Burns and J. Rozière, *J. Mater. Chem.*, 1999, **9**, 3125–3130.
- 14 F. Z. Forgeng, *Am. Mineral.*, 1960, **45**, 946–959.
- 15 International Centre for Diffraction Data (ICDD).
- 16 M. M. Thackeray, *Prog. Solid State Chem.*, 1997, **25**, 1.